Intersubband optical absorption in coupled quantum wells under an applied electric field

Perng-fei Yuh and K. L. Wang
Device Research Laboratory, Department of Electrical Engineering, University of California, Los Angeles, California 90024-1600
(Received 18 March 1988)

The very large tunability of the transition energy when an electric field is applied is found in the intersubband optical transition in two strongly coupled semiconductor quantum wells. The energy of the absorption peak can shift to red or blue and is very sensitive to the electric field, in contrast to the single-well case, which has only a small blue shift. The oscillator strengths and the selection rule depend on the degree of coupling and are quite different from the single-well case. The method we use to characterize the energy levels and the wave functions of the coupled quantum wells has several advantages over the previous theoretical calculations in that the effective-mass difference, the finiteness of the barrier height, and arbitrary structure of the quantum wells can be taken into account by using a transfer-matrix technique.

I. INTRODUCTION

The electric field dependence of the absorption coefficient in semiconductor quantum wells and superlattices has been studied extensively for possible electro-optical applications.[1-4] The exciton absorption peak of the interband transition (valence-to-conduction-band transition) in quantum-wells shifts to long wavelength (red shift) when the electric field is applied and is known as the quantum confined Stark effect. The quantum confined Stark effect in quantum wells is more significant than the Franz-Keldysh effect in the bulk semiconductor due to the confinement of the wave functions in the quantum wells.[3] On the other hand, the absorption edge of the intersubband transition (subband to subband transitions within the conduction band) in quantum wells shift to short wavelength (blue shift) under an applied electric field.[5,6] This intersubband Stark shift is small and cannot be used in optical modulation applications since the relative energies of the sublevels in a single well do not change much by the electric field.

The energy levels originated from different wells in coupled quantum wells, however, can be tuned individually by applying electric field. The strength of this interwell transition is small because the wave functions are partially overlapped.[7] The coupled quantum wells are defined as the quantum-well structure comprising more than one quantum well with interwell spacings and barriers sufficiently small so that significant amount of interaction takes place.[8] The energy states and wave functions of the coupled quantum wells in the absence of electric field were calculated by several authors.[8-10] We have calculated the energy states for a superlattice consisting of coupled-well basis.[11] Experimental investigation of the interband transition of the coupled quantum wells is also carried out.[7,12-14]

In this paper a formalism of the dispersion relation is developed for a general quantum well structure in the presence of the electric field. The effective-mass difference, coupling of the conduction band to the valence and split-off bands, and the finite height of the barriers are also taken into account. As a special case, the intersubband optical transitions in coupled quantum wells are analyzed by this approach. The Stark shift in the coupled wells is considerably larger than that in the single-well case while the oscillator strength is smaller for the former, depending on the degree of coupling. The selection rule also depend on how the wells are coupled. For example, the $1\rightarrow 3$ transition, which is forbidden in the single-well case, is possible in the coupled well case.

II. METHOD

The dispersion relation of an isolated quantum well is derived here. Figure 1 shows the conduction-band edge of an arbitrary quantum-well structure consisting of a finite number of layers with the total length L. The quantum-well structure is bounded by two infinitely thick potential barriers with height eV_l and eV_r on the left and right, respectively. The energies of interest are between the bottom of the wells and the minimum of eV_l and eV_r. The wave functions Ψ_l and Ψ_r on the left and right contacts, respectively, are

$$\Psi_l = Ae^{\kappa_l z}, \quad z \le 0$$
$$\Psi_r = Be^{-\kappa_r (z-L)}, z \ge L \tag{1}$$

where

$$\kappa_l^2 = -(2m_l^*/\hbar^2)(E - eV_l - E_\parallel) ,$$
$$\kappa_r^2 = -(2m_r^*/\hbar^2)(E - eV_r - E_\parallel) ,$$

E is the total energy and $E_\parallel = \hbar^2 k_\parallel^2/2m^*$, $k_\parallel$ is the wave vector normal to the z direction, and m^* is the effective mass in the corresponding region. Using the transfer-matrix technique,[15] Ψ_l and Ψ_r are related by

$$\begin{bmatrix} \Psi_r \\ \hline \Psi_r'/m_r \end{bmatrix} = S(L,0) \begin{bmatrix} \Psi_l \\ \hline \Psi_l'/m_l \end{bmatrix} , \tag{2}$$

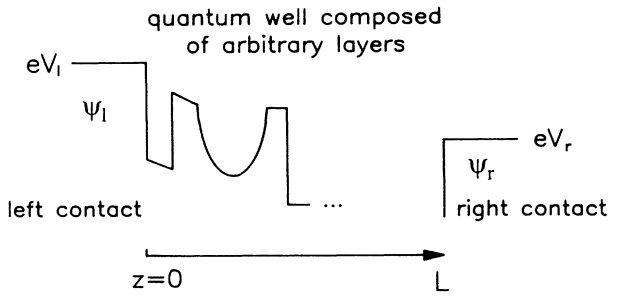

FIG. 1. Conduction-band edge of an arbitrary quantum well consisting of a finite number of layers with the total length L. Ψ_l and Ψ_r are conduction-band envelope functions along the z direction for the left and right contacts with potential eV_l and eV_r, respectively.

where S is a 2×2 transfer matrix. From Eqs. (1) and (2), the constant A and B can be eliminated and the dispersion relation is readily obtained as

$$-\frac{m_r^*}{\kappa_r}=\frac{S_{11}+(\kappa_l/m_l^*)S_{12}}{S_{21}+(\kappa_l/m_l^*)S_{22}} . \tag{3}$$

In calculating an arbitrary potential, the quantum well is divided into several sublayers. Each sublayer contains only a linear potential (tilted or constant). The transfer matrix S is the product of transfer matrices of the sublayers. The explicit expressions of the subtransfer matrix are given in Ref. 11 for a linear potential by the effective mass, two- and three-band models, respectively. The dispersion relations for two- and three-band models are obtained by substituting κ/m^* in Eq. (3) with

$$\begin{aligned}&\frac{\kappa}{m^*}\rightarrow\frac{\kappa}{E-V_p} ,\\ &\frac{\kappa}{m^*}\rightarrow\kappa\left[\frac{2}{E-V_p}+\frac{1}{E-V_o}\right] ,\end{aligned} \tag{4}$$

where V_p and V_o are the light-hole band and split-off band maximum, respectively.[11] The wave functions can be constructed once the energy states are determined.

The absorption coefficient of the intersubband transition from initial state n to the final state n' in the dipole approximation is given by

$$\alpha=\frac{\pi e^2\hbar c\mu_0}{2m^*n_r}f_{n'n}J_{n'n}(\omega)\times\Delta N , \tag{5}$$

where μ_0 is the permeability and c is the speed of light. The index of refraction n_r and the effective mass m^* are considered to be the average values in the quantum-well structure. The oscillator strength $f_{n'n}$ is given by

$$f_{n'n}=\frac{2}{m^*\hbar\omega}P_{n'n}^2=\frac{2m^*}{\hbar^2}E_g\langle n'\mid z\mid n\rangle^2 , \tag{6}$$

where $P_{n'n}$ is the momentum matrix element and $E_g=E_{n'}-E_n$ is the transition energy. The joint density of states $J_{n'n}$ in intersubband transitions is a δ function

$$J_{n'n}=2\delta(\hbar\omega-E_g) .$$

The broadening effect can be incorporated by experimental linewidth and then the density of states can be written as

$$J_{n'n}=\frac{2}{\pi}\frac{\hbar/T_2}{(E_g-\hbar\omega)^2+(\hbar/T_2)^2} , \tag{7}$$

where T_2 is of the order 10^{-13} sec by recent experiments.[5,16] The population difference ΔN of the initial state to the final state at finite temperature can be obtained,

$$\Delta N=N_n-N_{n'}=\frac{4\pi m^*}{h^2L}kT\ln\frac{1+e^{-(E_n-E_f)/kT}}{1+e^{-(E_n-E_f)/kT}} , \tag{8}$$

where L is the width of the quantum well and E_f is the Fermi energy. The peak absorption occurs at $\hbar\omega=E_g$ and is

$$\alpha=(4.3686\times10^4)f_{n'n}\frac{T_2}{10^{-13}\text{ sec}}\frac{\Delta N}{10^{18}\text{ cm}^{-3}}(\text{cm}^{-1}) \tag{9}$$

for the material parameters of GaAs.

III. RESULTS

The coupled quantum well structure comprising two wells A and B of dimension $W_A=100$ Å (35 monolayers) and $W_B=50$ Å (17 monolayers) and a barrier of dimension 30 Å (11 monolayers) inserted between A and B is investigated. This coupled-quantum-well structure is bounded by thick n^+ barriers such that the voltage drops only in the wells and the thin barrier. All the wells are assumed GaAs and the barriers $Al_{0.3}Ga_{0.7}As$. The 0.6:0.4 rule is used for the ratio of the conduction-band offset to the valence-band offset in $Al_xGa_{1-x}/GaAs$ heterojunctions.

In the discussion that follows, first the energy states and wave functions are calculated to illustrate how the wells are coupled. It is instructive to relate the energy states of the double well coupling case to the original single-well states. The term "interwell transition" refers to the intersubband transition whose initial state and final state are originated from different wells, while the term "intrawell transition" is for the transition between two states in the same well. The transition energy of the interwell transition is a strong function of the applied electric field. However, the oscillator strength of the interwell transition is in general smaller than that of the intrawell transition. The oscillator strength as a function of the well dimension, the barrier dimension, and the electric field is discussed secondly.

A. Energy states and wave functions

The energy states versus the well dimension of the B well is shown in Fig. 2(a). The two states at around 30 and 120 meV are originated from the A well and are labeled as $n_A=1_A$, and 2_A in Fig. 2. The three falling states come from the B well and are labeled as $n_B=1_B$, 2_B, and 3_B. For example, the $1\rightarrow2$ transition corre-

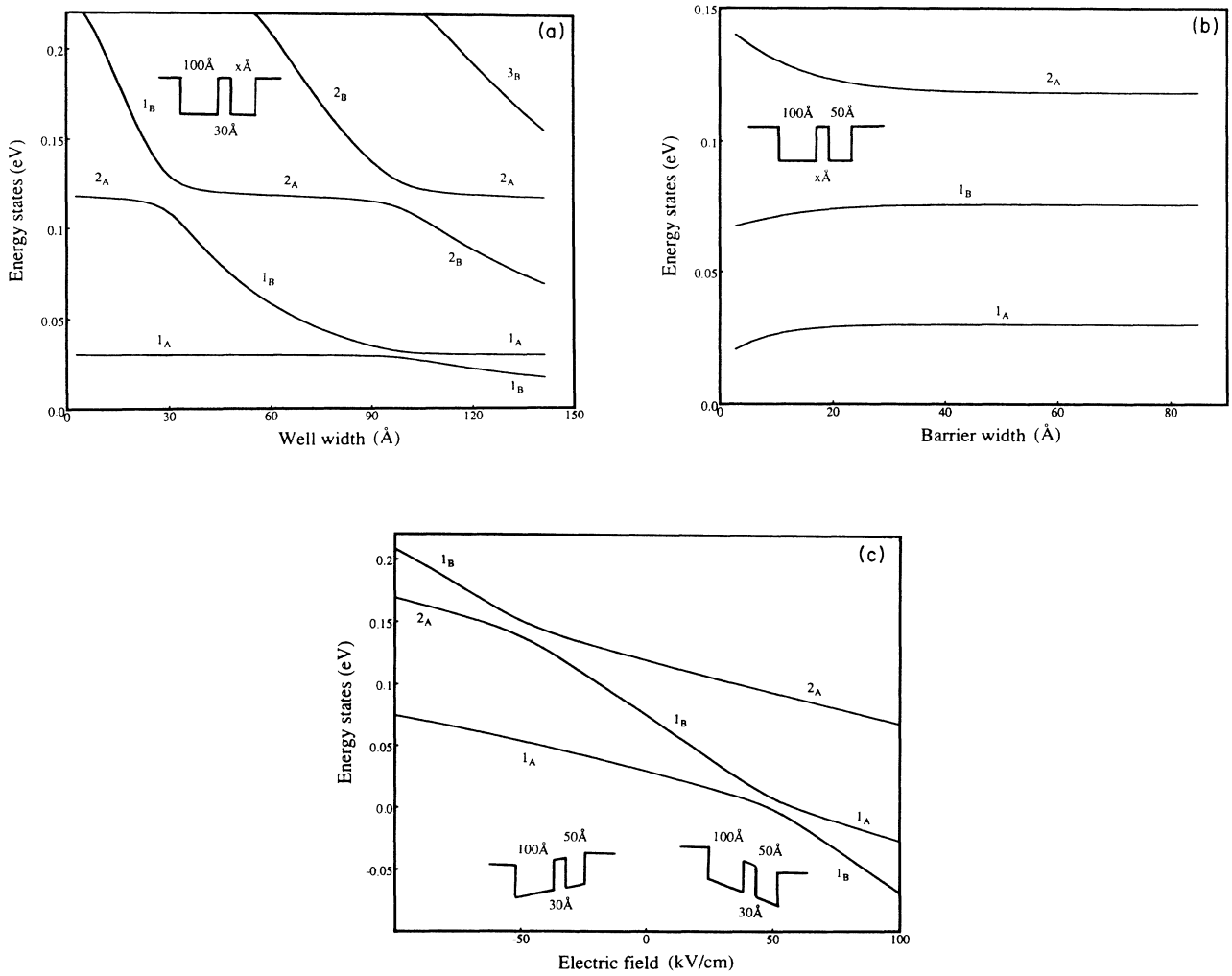

FIG. 2. Energy states as a function of (a) the well width, (b) the barrier width, and (c) the applied electric field for the coupled quantum wells comprising two wells A and B and a thin barrier in between. (a) Energy states as a function of the width of the B well when the A well is 100 Å and thin barrier is 30 Å. The energy states originated from the A well are labeled as $n_A = 1_A$ and 2_A and those from the B well are labeled as $n_B = 1_B$, 2_B and 3_B in order to distinguish the interwell transitions from the intrawell transitions. (b) Energy states as a function of the width of the thin barrier when the A well is 100 Å and B well is 50 Å. (c) Energy states as a function of the electric field when the A well is 100 Å, the B well is 50 Å, and thin barrier is 30 Å. The 1_B state intersects the 2_A state at the field -50 kV/cm, while it intersects the 1_A states at 50 kV/cm. The transition energies of the $1_A \rightarrow 1_B$ and the $1_B \rightarrow 2_A$ transitions is very sensitive to the applied electric field.

sponds to the $1_A \rightarrow 1_B$ interwell transition when the B well is 50 Å while it corresponds to the $1_A \rightarrow 2_A$ intrawell transition when the B well is 20 Å.

The energy states versus the barrier dimension is shown in Fig. 2(b). The barrier dimension has small effect on the energy states when the barrier width is larger than 30 Å.

The electric field dependence of the energy states is shown in Fig. 2(c). The polarity of the electric field is shown in the inset. The energy states originated from the A well and the B well are labeled in a way as in Fig. 2(a). The transition energy of the $1_A \rightarrow 2_A$ intrawell transition does not change much by the electric field but the $1_A \rightarrow 1_B$ interwell transition does. Depending on the polarity of the applied field, the transition energy can shift to small energy (red shift), or large energy (blue shift).

Shift of the absorption peak as large as 75 meV is predicted for the interwell transition case (the $1_A \rightarrow 1_B$ or equivalently, the $1 \rightarrow 2$ transition between the field -50 and 50 kV/cm). For comparison, the single well case has only a shift of 1.6 meV under an applied field of 36 kV/cm.[5] According to the recent intersubband experiments,[16] the full width at half maximum (FWHM) of the absorption coefficient is about 19 meV, which is much smaller than the shift of this interwell transition in coupled quantum wells by applying an electric field.

The wave functions of the lowest three states are shown in Fig. 3, for the zero field, -50 and 50 kV/cm,

respectively. The wave function oscillates in its own original well and decays in the other well in the zero field or small field cases. Thus the overlap of the interwell wave functions is considerably smaller than that of the intrawell wave functions. The -50 kV/cm fields are chosen such that the 1_B and 2_A states are mixed, thus the

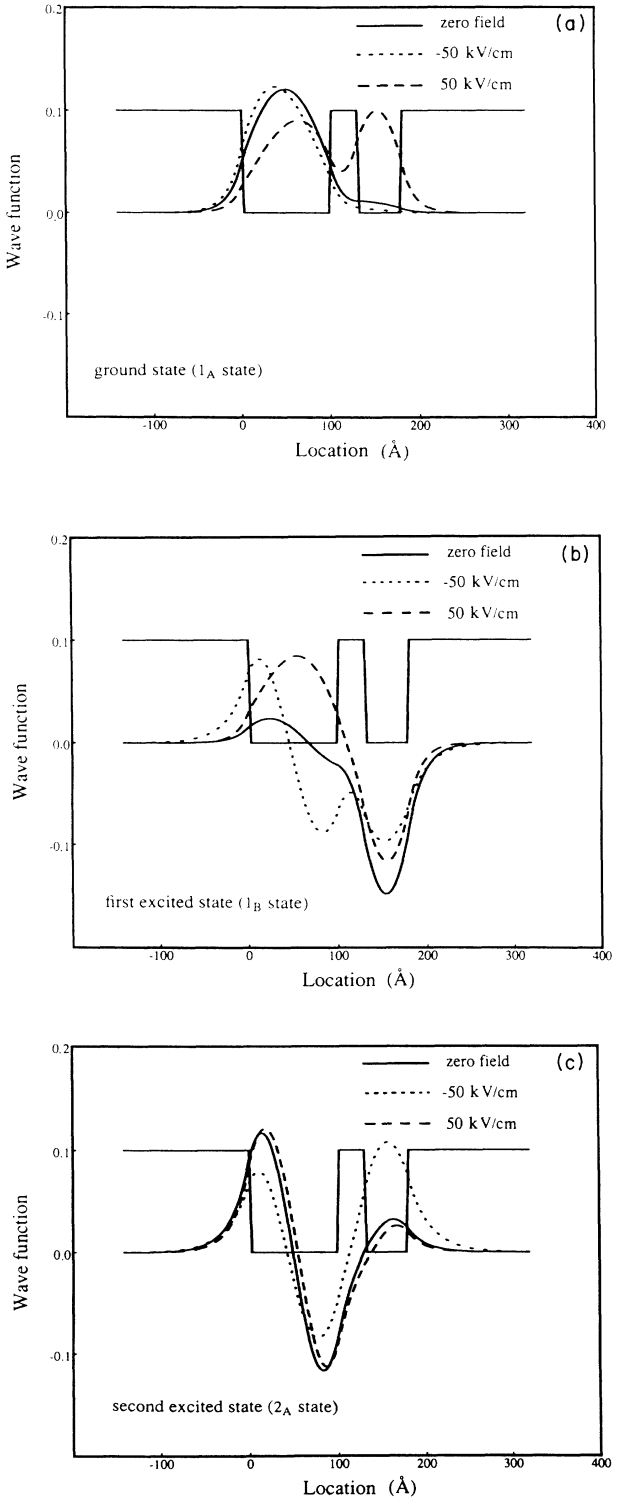

FIG. 3. Wave functions of the lowest three states in the coupled quantum wells described in Fig. 2(c) for the zero field, and ± 50 kV/cm, respectively.

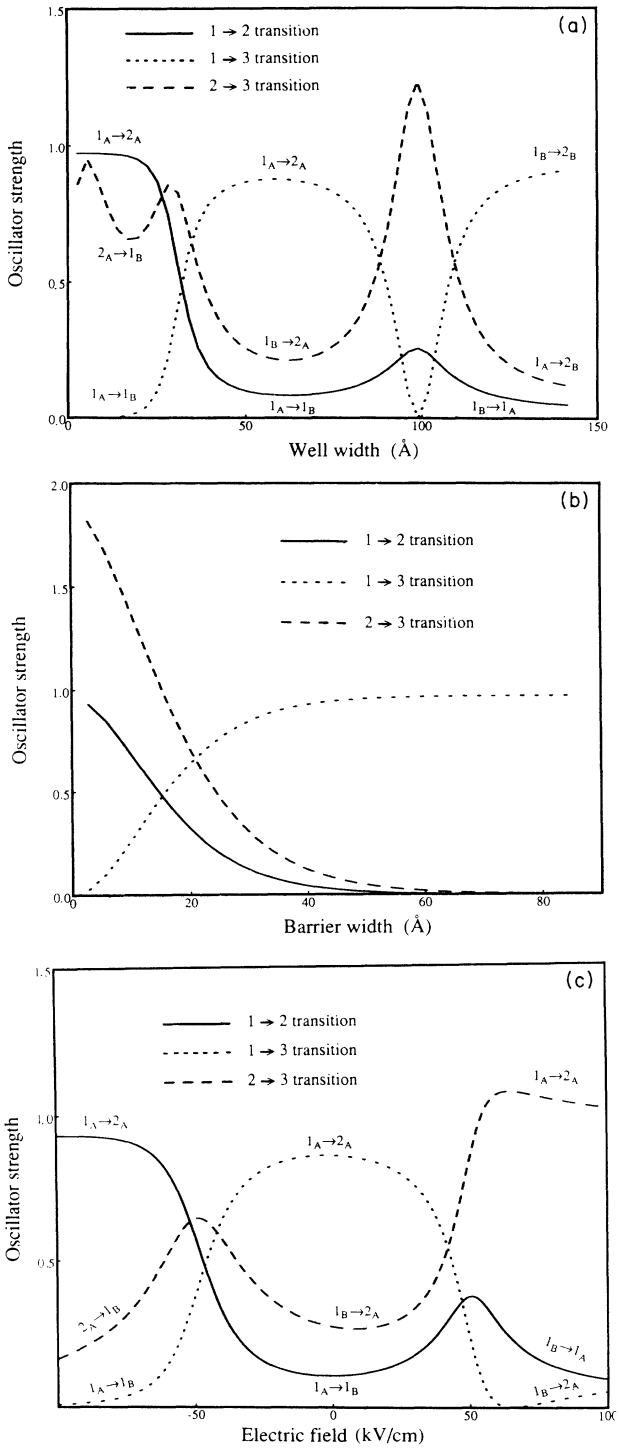

FIG. 4. Oscillator strength as a function of (a) the well width, (b) the barrier width, and (c) the applied electric field for the coupled quantum wells described in Fig. 2. (a) Oscillator strength as a function of the width of the B well. The oscillator strength is labeled in each section as the $1_A \rightarrow 1_B$, $1_A \rightarrow 2_A$ transitions, etc., according to the labeling in Fig. 2(a). The interwell transitions usually have small strength. (b) Oscillator strength as a function of the width of the thin barrier. The interwell transition $1_A \rightarrow 1_B$ has large strength when the thin barrier is smaller than 30 Å. (c) Oscillator strength as a function of the electric field. The oscillator strength is proportional to the absorption coefficient by Eq. (9).

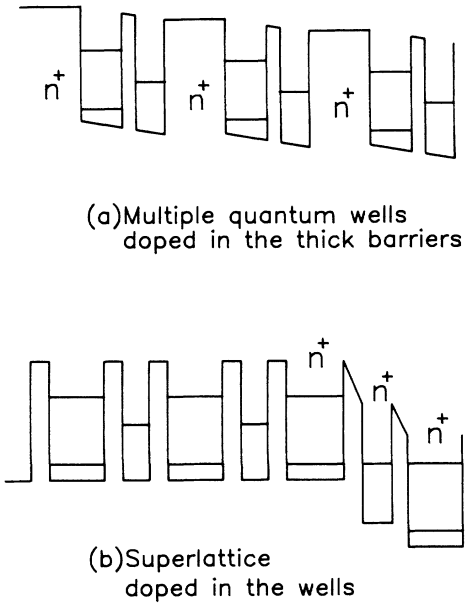

FIG. 5. Arrangement of the coupled quantum wells for electro-optical applications. (a) Multiple-quantum-well case: the undoped coupled quantum wells are inserted between heavily doped thick barriers. The electric field is distributed only in the coupled quantum wells. Thus the result in Sec. III can be directly applied. The peak absorption energy of the interwell transition can shift to red or blue by the electric field. (b) Superlattice case: a superlattice incorporates the coupled quantum wells as its basis. Only the well regions are heavily doped. High-electric-field domains are expanding well by well in the barrier regions so that the energy levels in each well are aligned. The transition energy of the interwell transition does not change with the electric field. But the absorption magnitude decreases as the domains expand since the absorbent wells available are decreasing.

wave functions of the 1_B and 2_A states are oscillatory in both wells. While at the field 50 kV/cm, the 1_B and 1_A states are mixed, where the wave functions of the 1_B and 1_A states are oscillatory in both wells.

B. Oscillator strength and absorption coefficient

To show that the intrawell transitions are usually stronger than the interwell transition, the oscillator strength versus the well dimension of the B well is plotted in Fig. 4(a). The $1\rightarrow2$, $1\rightarrow3$, and $2\rightarrow3$ transitions are labeled as $1_A\rightarrow1_B$, $1_B\rightarrow1_A$, $1_A\rightarrow2_A$, and $1_B\rightarrow2_A$ transitions in the corresponding regions in order to distinguish the interwell transition from the intrawell transitions. They are labeled according to the labeling in Fig. 2(a).

The thin barrier plays an important role for the interwell transitions. The oscillator strength versus barrier width is shown in Fig. 4(b). For a thinner barrier the two wells are strongly coupled and the interwell wave functions have large overlap and thus large oscillator strength while for a thicker barrier the two wells are decoupled and this approaches the single-well limit.

The oscillator strength versus electric field is shown in Fig. 4(c), where the transitions are labeled according to that in Fig. 2(c). The oscillator of the interwell transitions is 1 order of magnitude smaller than that of the intrawell transitions in the present example. The interwell oscillator strength peaks at the electric field when the energy levels are mixed.

IV. STRUCTURAL CONSIDERATION

In Sec. III we have assumed a uniform electric field applied only in the well regions and thin barrier. This is a good approximation if the contact barriers are heavily doped while the wells and the thin barrier are undoped, as schematically shown in Fig. 5(a). Multiple-coupled wells are required to enhance the absorption. The contact barriers should be thick enough (≥ 100 Å) in order to decoupled the individual coupled quantum wells. In this case both the blue shift and the red shift are possible.

The second possible arrangement is shown in Fig. 5(b), where the individual coupled wells are also coupled to the neighbors. The well regions should be heavily doped to ensure carriers accumulated in the ground state while the barriers are not doped. As the voltage is applied, the bands tend to align one by one,[17] as is shown schematically. Thus one may not expect an energy shift of the absorption peak, but the magnitude of the peak will drop since the number of absorbent wells available are decreasing as the number of aligned wells increases when the electric field is applied.

V. CONCLUSION

In conclusion, we have developed a formalism based on the transfer matrix to calculate the energies and wave functions in an arbitrary quantum-well structure. The intersubband optical transitions of the coupled quantum wells under an applied electric field are analyzed using this formalism. Very large Stark shift by the interwell transitions is predicted. However, the oscillator strength of the interwell transition is one order of magnitude smaller than the intrawell transition.

ACKNOWLEDGMENTS

The authors thank Dr. R. Karunasiri for the helpful discussions. This work is supported in part by U.S. Naval Research office, U.S. Army Research Office, and the Semiconductor Research Corporation.

[1]D. A. B. Miller, D. S. Chemla, T. C. Damen, A. C. Gossard, W. Wiegmann, T. H. Wood, and C. A. Burrus, Phys. Rev. B **32**, 1043 (1985).

[2]David A. B. Miller, Joseph S. Weiner, and D. S. Chemla IEEE J. Quantum Electron. **QE-22**, 1816 (1986).

[3]D. A. B. Miller, D. S. Chemla, and S. Schmitt-Rink, Phys. Rev. B **33**, 6976 (1986).

[4]B. Jogai and K. L. Wang, Phys. Rev. B **35**, 653 (1987).

[5]Alex Harwit and J. S. Harris, Jr., Appl. Phys. Lett. **50**, 685 (1987).
[6]D. Ahn and S. L. Chuang, Phys. Rev. B **35**, 4149 (1987).
[7]Y. J. Chen, Emil S. Koteles, B. Elman, and C. A. Armiento, Mater. Res. Soc. Symp. Proc. **102**, 571 (1988).
[8]Amnon Yariv, Chris Lindsey, and Uri Sivan, J. Appl. Phys. **58**, 3669 (1985).
[9]Roy Lang and Kenichi Nishi, Appl. Phys. Lett. **45**, 98 (1984).
[10]Herbert Kroemer and Hiroshi Okamoto, Jpn. J. Appl. Phys. **45**, 98 (1984).
[11]Perng-fei Yuh and K. L. Wang, Phys. Rev. B (to be published).
[12]Yasunori Tokuda, Teruhito Matsui, Kenzo Fujiwara, Noriaki Tsukada, and Takashi Nakayama, Appl. Phys. Lett. **51**, 209 (1987).
[13]H. Kawai, J. Kaneko, and N. Watanabe, J. Appl. Phys. **58**, 1263 (1985).
[14]H. Q. Le, J. J. Zayhowski, and W. D. Goodhue, Appl. Phys. Lett. **50**, 1518 (1987).
[15]M. O. Vassell, Johsnon Lee, and H. F. Lockwood, J. Appl. Phys. **54**, 5206 (1983).
[16]B. F. Levine, R. J. Malik, J. Walker, K. K. Choi, C. G. Bethea, D. A. Kleinman, and J. M. Vandenberg, Appl. Phys. Lett. **50**, 273 (1987).
[17]K. K. Choi, B. F. Levine, R. J. Malik, J. Walker, and C. G. Bethea, Phys. Rev. B **35**, 4172 (1987).